NÖHÜ Müh. Bilim. Derg. / NOHU J. Eng. Sci., Eng. Sci. 2023; 12(3), 973-982
Niğde Ömer Halisdemir Üniversitesi Mühendislik Bilimleri Dergisi
Niğde Ömer Halisdemir University Journal of Engineering Sciences
Araştırma makalesi / Research article
www.dergipark.org.tr/tr/pub/ngumuh / www.dergipark.org.tr/en/pub/ngumuh

The investigation of mill scale utilization as a reinforcement in aluminum matrix composites

Alüminyum matrisli kompozitlerde takviye olarak tufal kullanımının incelenmesi

Burak Birol[1,*]

[1] *Yıldız Technical University, Metallurgical and Materials Department, 34210, İstanbul Türkiye*

Abstract

Industrial waste is frequently utilized as reinforcing material in aluminum matrix composites (AMC) to improve their mechanical qualities. Mill Scale (MS), which is mainly composed of iron oxides, is obtained during the forming process of steel. In the present study, the utilization of MS as a reinforcement material in AMC was investigated. The MS obtained from a steel mill was initially pulverized by high-energy ball milling, and the milling parameters were studied. 20 hours of milling at 800 RPM provided the finest distribution of particle sizes with a d(0.5) value of 1.553 µm. The milled MS was blended with commercially pure aluminum with a ratio of 0-10 wt. % in a high-energy ball mill at 300 RPM for 60-300 min, then pressed and sintered for 2 h at 600-650 °C. It was observed that increasing milling time increases the hardness and lowers the porosity of the samples and increasing the temperature up to 615°C also decreases the porosity values. On the other hand, increasing reinforcement amount increases porosity up to ~10 vol. %, especially over 2.5 wt. %. However, increasing the MS amount results in higher hardness values and lower sample wear rates because of the harder particle reinforcement.

Keywords: Aluminium matrix composites, Mill scale, High energy ball milling, Hardness, Wear

Öz

Endüstriyel atıklar, alüminyum matrisli kompozitlerin mekanik özelliklerini arttırmak için takviye partikülleri olarak yaygın şekilde kullanılmaktadır. Çeliğin şekillendirilmesi sırasında esas olarak demir oksitlerden oluşan tufaller açığa çıkmaktadır. Bu çalışmada tufalin alüminyum matrisli kompozitlerde takviye malzemesi olarak kullanımı araştırılmıştır. İlk olarak bir çelikhaneden elde edilen tufal, yüksek enerjili bilyeli öğütme ile öğütülmüş ve öğütme parametreleri incelenmiştir. En iyi parçacık boyutu dağılımı (d(0.5)=1.553 µm), 800 RPM'de 20 saatlik öğütmeden elde edilmiştir. Öğütülmüş tufal, ticari olarak saf alüminyum ile ağırlıkça %0-10 oranında gezegen tipi bir bilyalı değirmende 300 RPM'de 60-300 dakika harmanlanmıştır, ardından preslenenerek 600-650 °C'de 2 saat sinterlenmiştir. Öğütme süresinin artmasının numunelerin sertliğini arttırıp gözenekliliğini azalttığı, sıcaklığın artmasının da gözeneklilik değerlerini 615°C'ye kadar azalttığı görülmüştür. Öte yandan, artan takviye miktarı gözenekliliği, özellikle ağırlıkça %2.5'in üzerinde, hacimce ~%10'a kadar artırmaktadır. Ancak daha sert tane takviye miktarı nedeniyle tufal miktarının artması sertlik değerlerini artırmakta ve numunelerin aşınma oranlarını düşürmektedir.

Anahtar kelimeler: Alüminyum matrisli kompozitler, Tufal, Yüksek enerjili bilyalı öğütme, Sertlik, Aşınma

1 Introduction

The requirements for high-strength properties in lightweight materials have led to the development of aluminum matrix composites (AMC) [1]. The reinforcement materials used in aluminum matrix composites can be in the form of fibers (carbon, glass, boron, etc.), short fibers/whiskers (graphite, mica, BN, TiB_2, etc.), or particles (oxides, carbides, etc.) [2–5]. Fiber reinforcements positively affect many properties like tensile strength and elastic modulus, while ceramic particle reinforcement materials such as SiC, TiC, Al_2O_3, etc., which lead with their high melting points and high hardness, improve the properties of AMCs like hardness and resistance to wear [1,6,7]. The application of ceramic particles as reinforcement attracts more attention due to the adjustable distribution, fraction, and particle size of the reinforcements. This results with adjusting the microstructural and mechanical properties of the AMCs [8,9].

The increasing amount of agricultural and industrial waste arises problems related to environmental pollution. Therefore, the use of these wastes has great potential in solving these problems. Some industrial wastes are also used in the production of many advanced materials, especially metal matrix composites, with their excellent physical and mechanical properties [1,6,10]. These wastes are thermal power plant fly ashes [1,11–15], red mud, [1,6,16–21], varying organic waste ashes like rice husk ashes [22], bamboo leaf ash [23], etc., iron and steelmaking slags [24,25], or hybrid composites that contain a combination of varying wastes waste and/or ceramic particles [26–29].

On the other hand, AMCs containing iron oxide are a relatively new subject and there are many studies investigating the properties of AMCs containing iron oxide.

* Sorumlu yazar / Corresponding author, e-posta / e-mail: bbirol@yildiz.edu.tr (B. Birol)
Geliş / Recieved: 24.12.2022 Kabul / Accepted: 10.04.2023 Yayımlanma / Published: 15.07.2023
doi: 10.28948/ngmuh.1223650

According to these studies, it was stated that iron oxide-reinforced composite materials increased the mechanical properties of the matrix while adding magnetic properties [30–38].

In the present study, the utilization of iron oxide-containing mill scales (MS) as reinforcement in commercially pure aluminum was investigated. To achieve this goal, initially, high-energy ball milling parameters of the MS were investigated. Subsequently, the finest particle size obtained MS was blended with aluminum between 1-10 wt. % in a high-energy ball mill. Then the mixtures were compacted and sintered under argon flow to determine the optimum parameters. The produced AMC products were characterized by optical microscopy. Additionally, the influence of reinforcing particle concentration on the AMCs' hardness and wear characteristics was examined.

2 Material and methods

2.1 Preparation of the samples

To prepare the AMC samples, commercially pure aluminum with a particle size of less than 125 µm and MS containing 69.95 wt. % of total iron (Fe_T) were utilized as raw materials. The phases that are present in the MS were determined by a Panalytical X'PertPro XRD equipment with Cu-Kα radiation. The obtained raw materials were initially dried at 105 °C for 2 h. Then the MS was crushed and ground for 1 h in a conventional ball mill. The ground MS were sieved under 500 µm and to investigate the high energy ball milling properties, the sieved MS was placed in stainless steel vials containing stainless steel balls with 10 mm diameter (10:1 ball/powder ratio) and ground in a DECO-PBMV-0.4 L planetary ball mill at 300, 500 and 800 r/min (RPM) velocities for 5, 10 and 20 h. To eliminate the overheating of the vials, the milling was paused for 5 min at 30 min intervals. The particle size distribution after each milling process was determined by Malvern Hydro 2000MU Mastersizer.

The Al particles and high-energy ball-milled MS that has the finest average particle size (*d(0.5)*=1.553 µm) were blended with MS ratios of 1, 2.5, 5, and 10 wt. %. (MS1, MS2.5, MS5 and MS10, respectively) by a planetary ball-mill at 300 RPM for 1, 3, and 5 h with a 10:1 ball-to-powder ratio. In order to prevent Al oxidation during the blending tests, 1 wt. % of stearic acid was used as a process controlling agent (PCA).

Using a uniaxial die, 3 g of ball-milled specimens were compressed for 5 min at 575 MPa to obtain cylindrical agglomerates with a 15 mm diameter. Then, they were sintered to produce AMCs at 600, 615, 625, and 650 °C. The sintering process was carried out in a tube furnace under an argon atmosphere with a determined heating regime to remove the stearic acid and prevent cracking in the samples. For the initial heating, stearic acid was removed by heating the samples at a rate of 3 °C/min to 400 °C and holding it there for 30 min. The samples were then heated at a rate of 5°C/min to sintering temperature and held for 2h at the sintering temperature and finally cooled in the furnace.

2.2 Characterization of the AMCs

Visual inspection, density measurements (ρ_m), and the porosity values (in vol. %) calculated using the Archimedes' principle as a mean of four measurements were used to evaluate the characteristics of the AMC samples. To be able to determine the porosity values, initially, theoretical density (ρ_T) was calculated with Equation 1 [4,39].

$$\rho_T = m_{Al} \times \rho_{Al} + m_{MS} \times \rho_{MS} \quad (1)$$

where, accordingly, m and ρ define the weight percentage and density of the components. The density of the mill scale (ρ_{MS}) was measured as 5.72 g/cm^3 by a Quantachrome Ultrapyc 1200e helium pycnometer. The theoretical density of the aluminum (ρ_{Al}) was considered as 2.7 g/cm^3. Equation 2 was used to determine the AMCs' porosity [4,39].

$$\text{Porosity (\% vol.)} = 100 \times \left(1 - (\rho_T/\rho_m)\right) \quad (2)$$

The BMS 200-RBOV Brinell hardness test apparatus, which has a 2.5 mm ball diameter and a 62.5 kgf force, was used to determine the hardness of the AMCs.

Wear tests were applied to AMC samples by pin-on-disc wear equipment according to ASTM G133-05. A 100Cr6 steel ball with an 840 HV hardness and of 10 mm diameter was used for the tests. The samples were subjected to a 10N force that was applied while sliding over a 300-meter distance at a speed of 0.05 m/s. Initially, volume loss (m^3) was calculated from Equation 3.

$$\Delta V = 1000 \times \left(W_i - W_f\right)/\rho \quad (3)$$

ΔV is the volume loss, W_i and W_f, are the initial, and final weight, and ρ is density of the sample. Then, a specific wear rate (k_S) value (m^3/N.m) was calculated by using Equation 4.

$$k_S = \Delta V/(L \times d) \quad (4)$$

Here, d is the sliding distance, and L is the standard load. A Jeol JSM 5410LV Scanning Electron Microscope (SEM) and a Nikon Eclipse MA100 Microscope were used for the microstructural characterization of the AMCs.

3 Results and discussions

3.1 Characterization of MS after high-energy ball-milling

The XRD analysis of the MS is presented in Figure 1, where Fe_2O_3, Fe_3O_4, and FeO phases were observed.
Figure 2 (a) illustrates the particle size distribution of MS after initial grinding and sieving, and high-energy ball-milled products after 5, 10, and 20 h with 300, 500, and 800 RPM velocities. *d(0.1)* and *d(0.9)* values which give an opinion about the fine and coarse particle size distribution, respectively, and *d(0.5)*, which is the average particle size for all the ball-milling parameter variation are also given in Figure 2 (b). The conventional ball milling process for 1 h

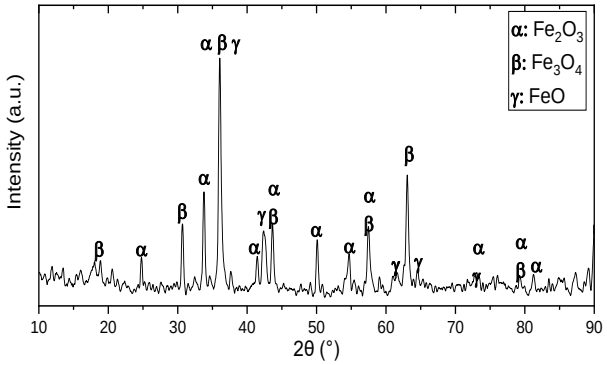

Figure 1. XRD patterns of MS

had particle sizes of *d(0.1)*, *d(0.5)*, and *d(0.9)* as 32.912, 93.564, and 412,923 µm, respectively. Both increasing milling speed and time lowered all these values as shown in Figure 2. When 5 h of milling is examined in detail, increasing milling speed lowered the *d(0.1)* and *d(0.9)* proportionally. On the other hand, the average particle size (*d(0.5)*) did not change considerably and it can be deduced that milling speed does not significantly affect the average particle size. Additionally, 300 RPM and 500 RPM milling speeds resulted in a more homogenous particle size distribution after 5h of milling, but at 800 RPM speed most of the particles coagulated at nearly 100 µm, while very fine particles, which were not encountered at the lower milling velocities, also formed.

After 10 and 20h of milling time at all velocities, the amount of bigger particles lowered and the number of particles less than 1 µm increased, especially at 800 RPM speed. Because the lowest particle size distribution was observed at 800 RPM for 20 h of milling time, the AMCs were produced with the MS particles that were produced with these parameters.

3.2 Investigation of the AMC production parameters

To determine the optimum sintering temperature, composite powders were prepared by blending as obtained Al powder with 1 wt. % stearic acid addition and a reinforcement ratio of 1, 2.5, 5, and 10 wt. %. Blending was conducted in a planetary ball mill at 300 RPM speed for 3 hours with a 10:1 ball-to-powder ratio. Then, pellets were pressed under 575 MPa pressure for 5 min and then sintered for 2 hours at 600, 615, 625, and 650 °C. Figure 3 (a) and (b), respectively, present the macrographs, theoretical density, observed density, and porosity values of the samples produced by Equations 1 and 2.

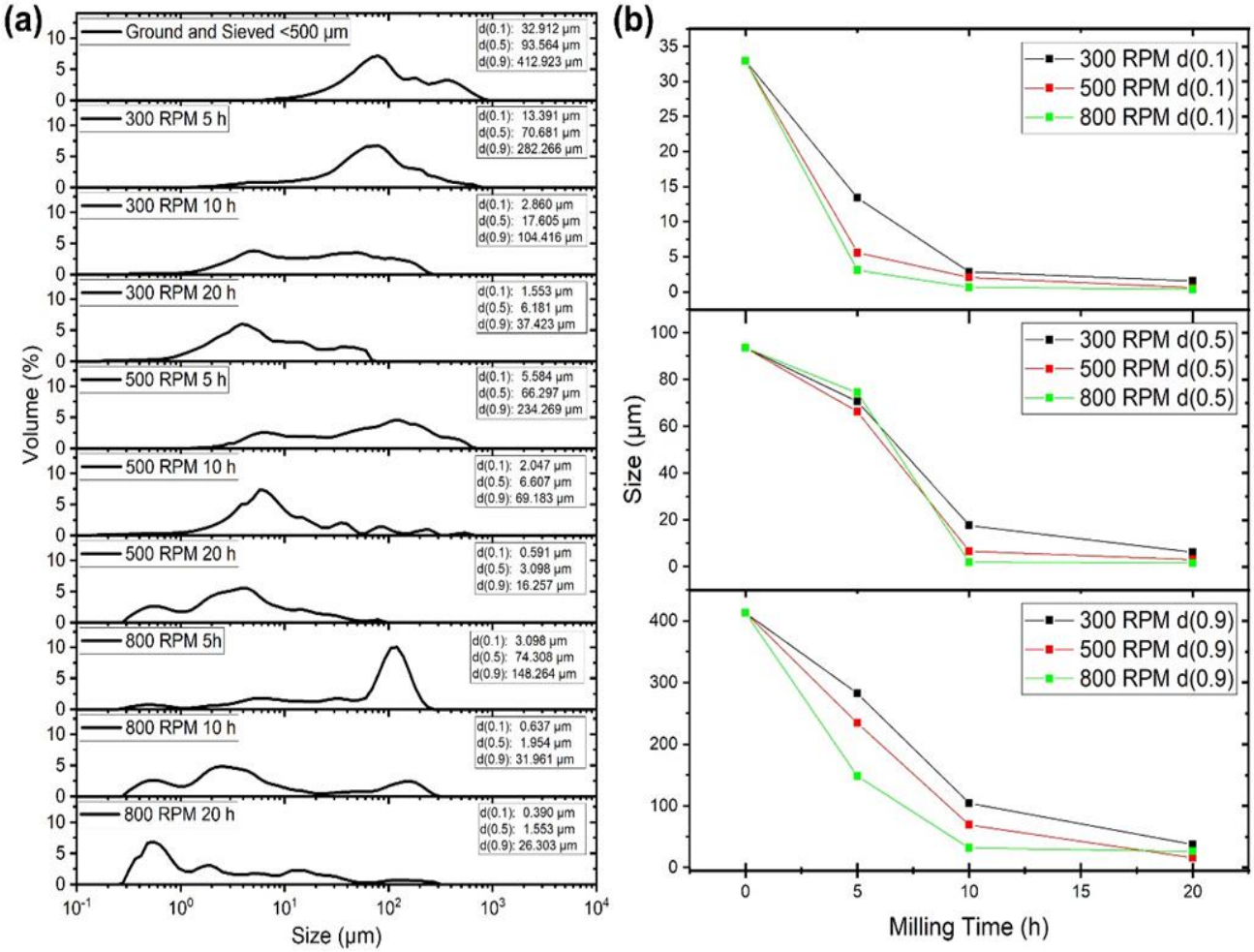

Figure 2. (a) Particle Size Distribution and (b) the change of *d(0.1)*, *d(0.5)*, and *d(0.9)* of MS after ball milling for 1h and sieving and high-energy ball milled products after 5, 10, and 20h with 300, 500 and 800 RPM velocities

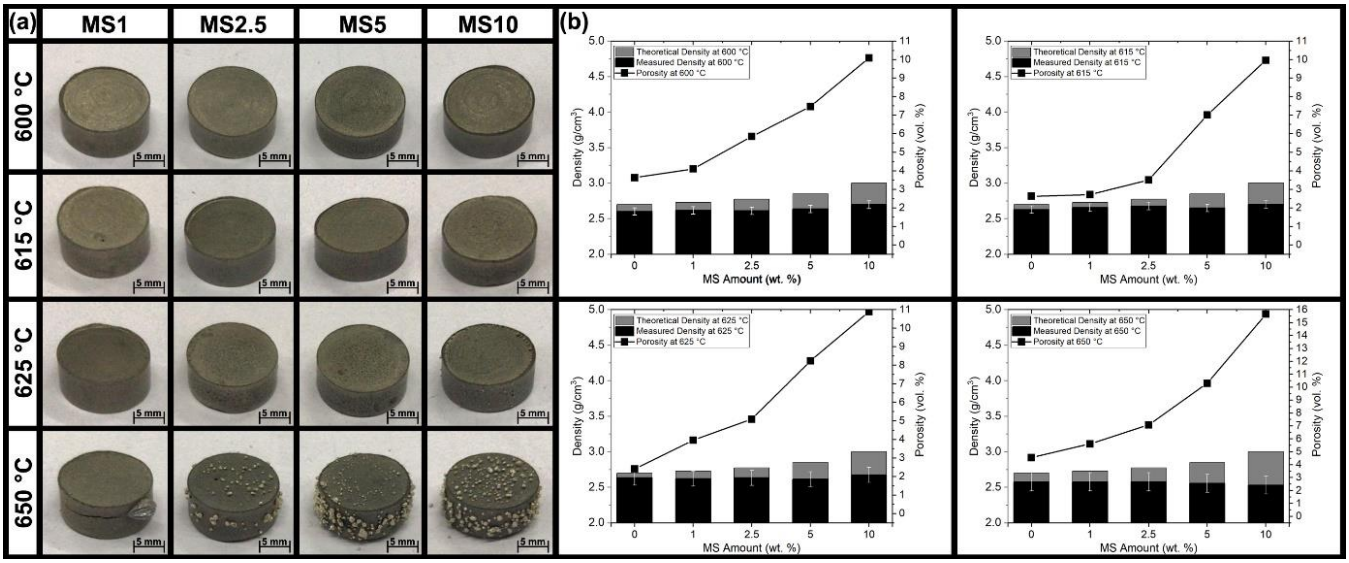

Figure 3. (a) The macrographs and (b) theoretical density, measured density, and determined porosity values of the samples containing 0, 1, 2.5, 5, and 10 wt. %. MS sintered at 600, 615, 625, and 650 °C

The macrographs of the samples (Figure 3 (a)), which were sintered at 600, 615, and 625 °C, revealed a smooth metallic surface. However, when examined in detail, some black dots began to appear on the samples sintered at 625 °C. Additionally, on the samples that were sintered at 650 °C, metallic droplets were observed on the composite structure. Also, in Figure 3 (b), as the sintering temperature is raised, there is a slight decrease in porosity up to 615 °C, a slight rise at 625 °C, and a significant increase at 650 °C. The partial melting of the Al particles over 615 °C can explain this behavior. Due to the low wetting of molten Al, these molten particles penetrate through the structure and coalesces on the surface of the samples as droplets by evacuating the area they were present and increasing the porosity of the samples. Generally, the sintering was applied up to 615 °C in the literature, regardless of the sintering method (conventional, spark plasma, microwave sintering methods, etc.) and it was reported that increasing temperature increases the density and accordingly lowers the porosity of the AMC [40–47]. Especially at temperatures near the matrix metal's melting point, compact swelling of the matrix metal occurs and the liquid exudes from pores as explained by German et al. [48].

Figure 3 (b) also shows that as the amount of reinforcement rose, the range between theoretical and measured densities widened, which also affected the samples' porosity values for all the sintering temperatures. According to the literature, it is expected for the porosity to increase as the amount of reinforcement increases [4,6,49,50]. Birol et al. [4] and Maleki et al. [50] asserted that aggregation and uneven distribution of the reinforcing are responsible for the porosity increase. Additionally, Calin et al. [51] claim that the liquid aluminum does not wet the reinforcing surfaces and it is responsible for the development of porosity in stir-cast parts. The creation of porosity and clustering of the reinforcing material as a result of the hydrated oxide coating on metal powders was documented by Borgohain et al. [49].

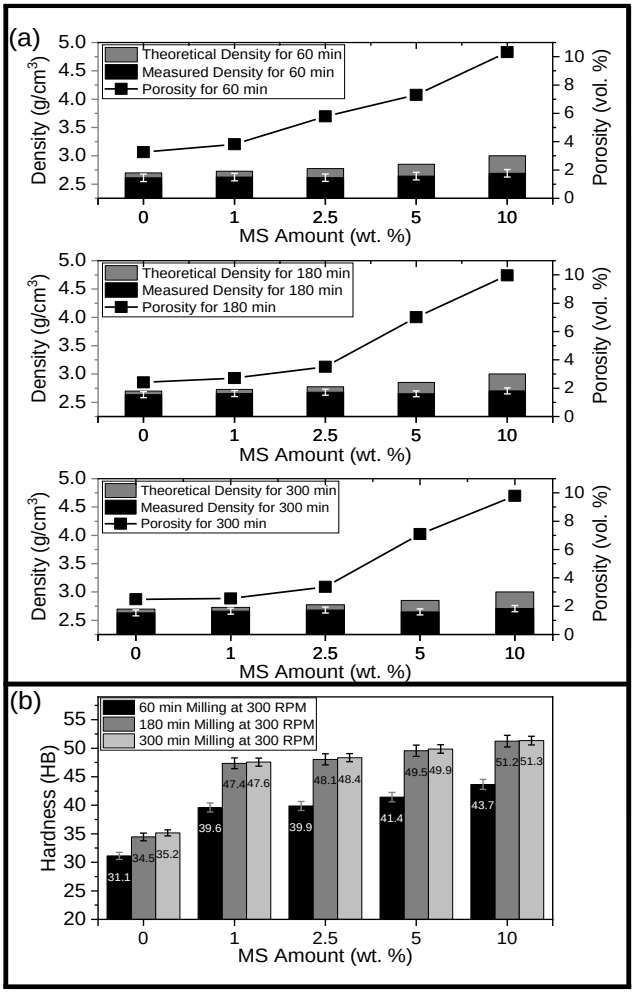

Figure 4. (a) Theoretical density, measured density, determined porosity values, and (b) hardness of the samples containing 0, 1, 2.5, 5, and 10% wt. MS, blended with high energy ball milling at 300 RPM for 1, 3, and 5 h and sintered at 615 °C

Figure 4 (a) illustrates the porosity and Brinell hardness variation of the samples blended in a planetary ball mill at 300 RPM for 1, 3, and 5 h and sintered at 615 °C. According to the results, the porosity values are strongly influenced by the blending time. Up to 2.5 % of the reinforcement amount increasing blending time from 1h to 3h, a nearly 25 – 40 % of porosity reduction was obtained. However, higher reinforcement amounts resulted with a porosity reduction of nearly 4 %. On the other hand, a slight decrease in the porosity (~4 %) for all the MS amounts was observed when the blending time was expanded from 3 to 5 h. As given in Figure 4 (b) increasing the reinforcement amount increased the hardness of the specimens, however, milling time exclusively played an important role in the hardness values. Extending the milling period from 1 to 3 h resulted with a significant increment in hardness where 5 h of milling time displayed a minor effect, just as observed in the porosity values.

An akin phenomenon was noted by Cabeza et al. [52] where work hardening of aluminum occurred after 3 h of milling and the hardness value of pure aluminum had risen from 31.1 to 34.5 HB. However, after 5 h of milling, the hardness had only increased to 35.1 HB. Moreover, the addition of only 1 % of MS to the AMC, elevated the hardness values for 1, 3, and 5 h of milling, 39.6, 47.4, and 47.6 HB, respectively. This significant increment was obtained due to the work hardening of aluminum, especially for 3h and 5 h milling, and grain refinement of the matrix due to interactions between reinforcement particles and grain boundaries acting as pinning points, delaying, or preventing grain growth. This results in fine matrix grain microstructure and higher mechanical properties as mentioned in the literature [3,53–55]. Additionally, the increasing amount of hard reinforcement particles in a composite material is well known to increase its hardness [4]. There is a linear increase with increasing reinforcing amount, as seen in Figure 4 (b).

3.3 Investigation of the MS amount influence on the microstructural and wear properties

Figure 5 exhibits the micrographs of the samples containing MS0, MS2.5, MS5, and MS10 blended at 300 RPM for 3h and sintered at 615 °C. The light grey areas are the Al matrix, the darker areas are the MS reinforcements, and the black areas are the voids. The porosity was examined between the Al grain boundaries in the sample MS0. Additionally, in sample MS2.5, the voids were discernible at the interface of the Al matrix and the reinforcing particles; as a result, no appreciable increase in porosity was found. On the other hand, the samples MS5 and MS10 demonstrate an elevation in the clustering of the particles in samples having more than 2.5% MS. This also increased the number of spaces between the reinforcing particles, which explains the marked increase in porosity values.

The wear data measured and obtained by Equations (3) and (4) are presented in Table 1 and Figure 6, respectively.

According to the wear test results, which were carried out under a 10N load for 300 m, the sample without MS had the greatest volume loss and specific wear rate values (MS0). A significantly lower k_S was found for the sample (MS1) which included 1 wt. % of MS. A linear decrease with the increasing MS amount was observed. Coefficient of friction (CoF) changes with the sliding distance reveal that especially over 200 m, the wear properties of the samples reached a steady-state condition and severe deformation was not observed. The lowest CoF values were obtained from the samples containing the highest MS amount. Moreover, according to Ozturk et al. [56] and Li et al. [57], hardness and wear resistance have a direct correlation, which was also observed in the current study.

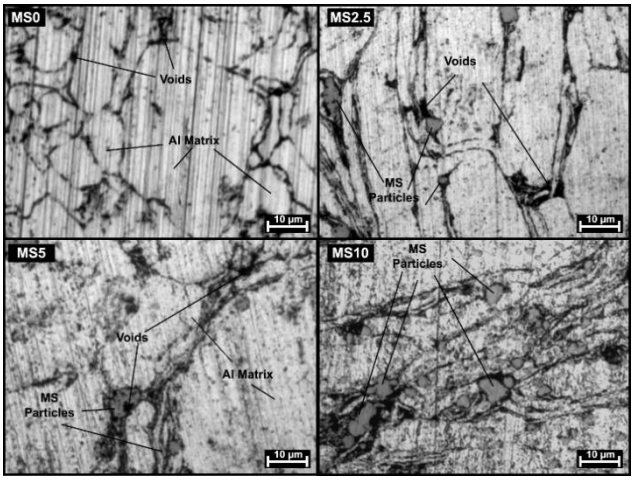

Figure 5. The micrographs of the samples containing MS with 0, 2.5, 5, and 10 wt. %. amounts blended at 300 RPM for 3h and sintered at 615 °C

Additionally, Figure 7 reveals the SEM micrographs of the worn surfaces of MS1, MS2.5, MS5, and MS10, respectively. On the worn surfaces of MS1 and MS2.5 (Figure 7 (a) and (b)), mainly delamination and plastic deformation were observed. Although some grooves and defragmented particles were present in both of these samples, the main wear mechanism can be accounted as adhesive wear [4,52].

Table 1 Wear data of the samples

	MS0	MS1	MS2.5	MS5	MS10
Initial Weight, W_i, g	2.8239	2.4699	2.3792	2.3149	2.8844
Final Weight, W_f, g	2.7853	2.4461	2.3609	2.3022	2.8801
Weight Loss, ΔW, g	0.0386	0.0238	0.0183	0.0127	0.0043
Density, ρ, kg/m^3	2629	2656	2678	2651	2703
Volume Loss, ΔV, m^3 x 10^{-9}	14.682	8.961	6.833	4.791	1.591
Specific Wear Rate, k_S, m^3/N.m x 10^{-12}	4.894	2.987	2.278	1.597	0.530

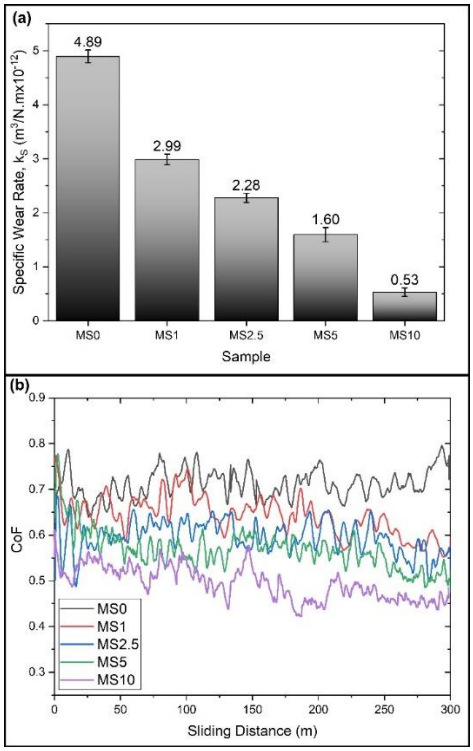

Figure 6. (a) Specific wear rate and (b) coefficient of friction (CoF) values of the samples

Additionally, the samples containing 5% and 10% MS, exhibit higher amounts of defragmented particles and deeper grooves as well as accumulated oxide particles throughout the worn surfaces as shown in Figure 7 (c) and (d). Thus, it may be claimed that these formations are indicative of abrasive wear as Mazahery et al. [58] explained. The harder reinforcement particles protrude out from the surface of the soft matrix as it wears. As the wear process progressed, some of these fragmented particles were re-embedded inside the soft matrix, but the rest were caught between the sample and the pin. As a result, there is abrasive activity between these broken-up and protruded particles. As a result, the wear rate lowers as the number of protruded particles (reinforcement particles) increases [1,4,58].

4 Conclusions

It was intended for the current study to examine the usability of mill scale, which is a waste obtained during the forming process of steel and mainly composed of iron oxides. To accomplish this goal, the mill scale obtained was ball milled and blended with commercially pure aluminum by using a planetary high-energy ball mill with different milling parameters. Then pressed and sintered at varying temperatures.

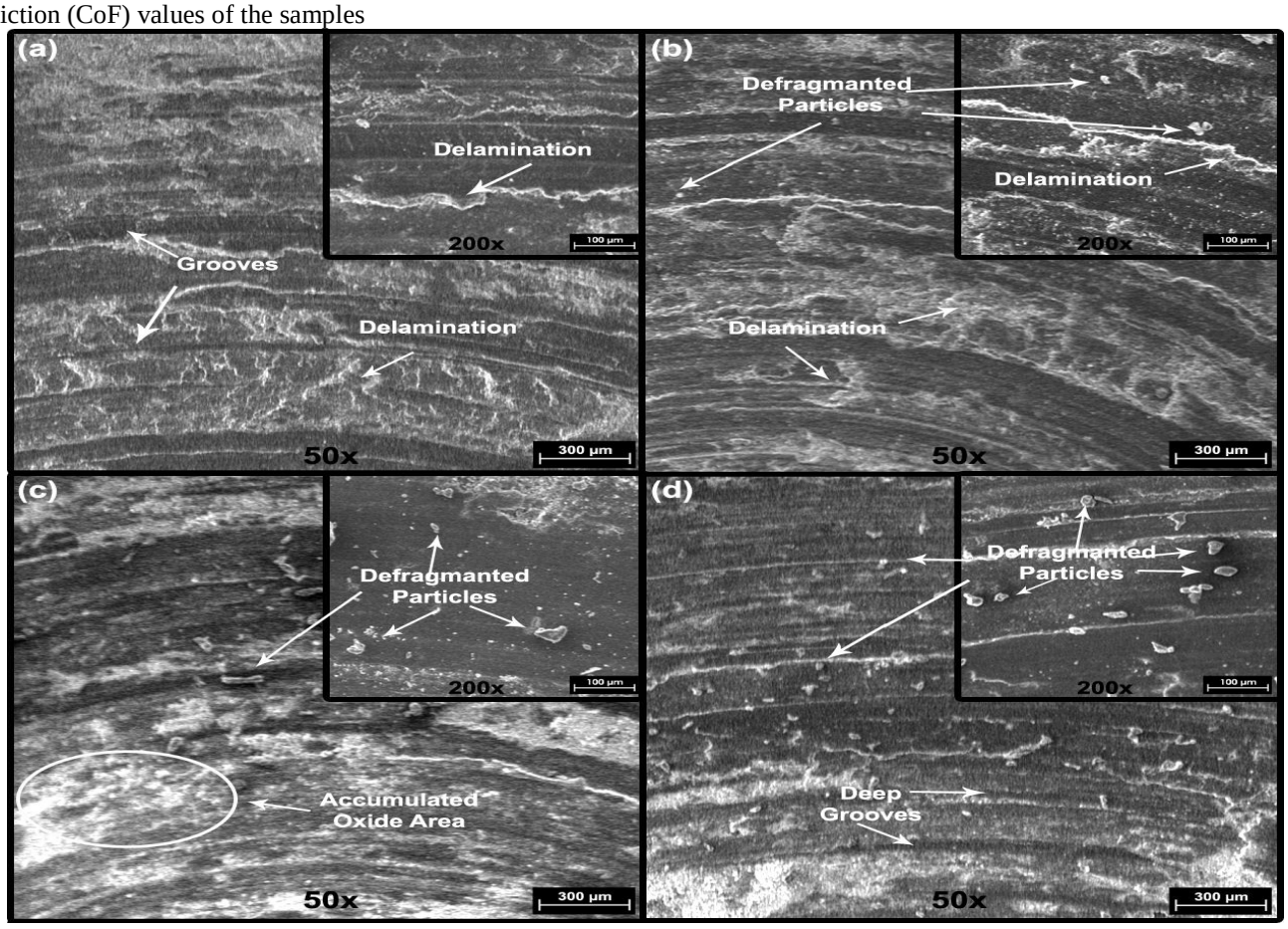

Figure 7 SEM micrographs of worn surfaces obtained from (a) M1, (b) M2.5, (c) M5, and (d) M10 with a magnification of 50x and 200x

Finally, the produced AMCs were characterized by Archimedes' principle, hardness, and wear tests. Depending on the results, the following statements were concluded;

1. Increasing ball milling rate and time, lowers the median particle size (d(0.5)) of the MS particles. At 800 RPM, lower milling times produce a non-homogenous particle size distribution where both bigger and very small particle sizes are present. However, increasing milling time grinds the bigger particles to obtain a final *d(0.5)* of 1.553 µm.
1. The sintering temperature has a positive role in the densification of the samples up to 615 °C. Over this temperature the aluminum particles begin to partially melt, leaving their original places into porosity and therefore densification lowers.
2. With the increasing blending time of ball-milled MS and aluminum at 300 RPM, increases the densification and hardness of all the samples. On the other hand, no significant differences were encountered between 180 and 300 min of milling time. It can be explained by the work hardening of aluminum and this mechanism affects the properties of the samples up to 180 min significantly, where the effectiveness of this mechanism is lower at blending times over 180 min.
3. The density of the samples is negatively impacted by the reinforcement amount, and the porosity rises with the increment of the reinforcement amount, due to the coagulation of the fine MS particles. On the other hand, reinforcement amount increment results in higher hardness values and wear resistance.
4. The wear resistance experiments reveal that up to 2.5% of reinforcement addition, the adhesive wear mechanism is dominant, while over this ratio abrasive wear mechanism is more prevailing.

Acknowledgement

This work was conducted with the support of the Yıldız Technical University, Metallurgical and Materials Engineering Department. Also, the author would like to acknowledge Samed GEZ for his assistance with the experiments and Rıdvan GECÜ for his comments on the wear data.

Conflict of interest

The authors declare that there is no conflict of interest.

Similarity rate (iThenticate): 19%

References

[1] M.O. Bodunrin, K.K. Alaneme, and L.H. Chown, Aluminium matrix hybrid composites: a review of reinforcement philosophies; mechanical, corrosion and tribological characteristics. Journal of Materials Research and Technology, 4(4), 434–45, 2015. https://doi.org/10.1016/j.jmrt.2015.05.003.

[2] R. Bauri and D. Yadav, Introduction to Metal Matrix Composites, Metal Matrix Composites by Friction Stir Processing, Elsevier, 2018, pp. 1–16

[3] A. Lakshmikanthan, S. Angadi, V. Malik, K.K. Saxena, C. Prakash, S. Dixit, and K.A. Mohammed, Mechanical and Tribological Properties of Aluminum-Based Metal-Matrix Composites. Materials, 15(17), 6111, 2022. https://doi.org/10.3390/ma15176111

[4] B. Birol, B. Süngü Misirlioğlu, and Ö. ÇAKIR, Investigation of magnetite concentrate utilization as reinforcement in aluminum matrix composites. Journal of Composite Materials, 56(25), 3897–910, 2022. https://doi.org/10.1177/00219983221124753

[5] C. Suryanarayana and N. Al-Aqeeli, Mechanically alloyed nanocomposites. Progress in Materials Science, 58(4), 383–502, 2013. https://doi.org/10.1016/j.pmatsci.2012.10.001

[6] N.K. Bhoi, H. Singh, and S. Pratap, Developments in the aluminum metal matrix composites reinforced by micro/nano particles – A review. Journal of Composite Materials, 54(6), 813–33, 2020. https://doi.org/10.1177/0021998319865307

[7] A. Lakshmikanthan, S. Angadi, V. Malik, K.K. Saxena, C. Prakash, S. Dixit, and K.A. Mohammed, Mechanical and Tribological Properties of Aluminum-Based Metal-Matrix Composites. Materials, 15(17), 6111, 2022. https://doi.org/10.3390/ma15176111

[8] L.A. Dobrzański, A. Włodarczyk, and M. Adamiak, The structure and properties of PM composite materials based on EN AW-2124 aluminum alloy reinforced with the BN or Al2O3 ceramic particles. Journal of Materials Processing Technology, 175(1–3), 186–91, 2006. https://doi.org/10.1016/j.jmatprotec.2005.04.031

[9] M. Rahimian, N. Parvin, and N. Ehsani, Investigation of particle size and amount of alumina on microstructure and mechanical properties of Al matrix composite made by powder metallurgy. Materials Science and Engineering: A, 527(4–5), 1031–8, 2010. https://doi.org/10.1016/j.msea.2009.09.034

[10] M.K. Gupta, P.K. Rakesh, and I. Singh, Application of Industrial Waste in Metal Matrix Composite. Journal of Polymer & Composites, 4(3), 27–34, 2016

[11] I. Dinaharan and E.T. Akinlabi, Low cost metal matrix composites based on aluminum, magnesium and copper reinforced with fly ash prepared using friction stir processing. Composites Communications, 9, 22–6, 2018. https://doi.org/10.1016/J.COCO.2018.04.007

[12] I. Dinaharan, R. Nelson, S.J. Vijay, and E.T. Akinlabi, Microstructure and wear characterization of aluminum matrix composites reinforced with industrial waste fly ash particulates synthesized by friction stir processing. Materials Characterization, 118, 149–58, 2016. https://doi.org/10.1016/j.matchar.2016.05.017

[13] I. Dinaharan and E.T. Akinlabi, Low cost metal matrix composites based on aluminum, magnesium and copper reinforced with fly ash prepared using friction stir processing. Composites Communications, 9, 22–6, 2018. https://doi.org/10.1016/J.COCO.2018.04.007

[14] T.P.D. Rajan, R.M. Pillai, B.C. Pai, K.G.

Satyanarayana, and P.K. Rohatgi, Fabrication and characterisation of Al-7Si-0.35Mg/fly ash metal matrix composites processed by different stir casting routes. Composites Science and Technology, 67(15–16), 3369–77, 2007. https://doi.org/10.1016/J.COMPSCITECH.2007.03.028

[15] V.K. Sharma, R.C. Singh, and R. Chaudhary, Effect of flyash particles with aluminium melt on the wear of aluminium metal matrix composites. Engineering Science and Technology, an International Journal, 20(4), 1318–23, 2017. https://doi.org/10.1016/J.JESTCH.2017.08.004

[16] N. Prasad, Dry Sliding Wear Behavior of Aluminium Matrix Composite Using Red Mud an Industrial Waste. International Research Journal of Pure and Applied Chemistry, 3(1), 59–74, 2013. https://doi.org/10.9734/IRJPAC/2014/2906

[17] C. Kar, B. Surekha, H. Jena, and S.D. Choudhury, Study of Influence of Process Parameters in Electric Discharge Machining of Aluminum – Red Mud Metal Matrix Composite. Procedia Manufacturing, 20, 392–9, 2018. https://doi.org/10.1016/J.PROMFG.2018.02.057

[18] Y.K. Singla, R. Chhibber, H. Bansal, and A. Kalra, Wear behavior of aluminum alloy 6061-based composites reinforced with SiC, Al2O3, and red mud: a comparative study. JOM, 67(9), 2160–9, 2015. https://doi.org/10.1007/s11837-015-1365-0

[19] P. Samal, R.K. Mandava, and P.R. Vundavilli, Dry sliding wear behavior of Al 6082 metal matrix composites reinforced with red mud particles. SN Applied Sciences, 2(2), 313, 2020. https://doi.org/10.1007/s42452-020-2136-2

[20] S. Rajesh, D. Devaraj, R. Sudhakara Pandian, and S. Rajakarunakaran, Multi-response optimization of machining parameters on red mud-based aluminum metal matrix composites in turning process. The International Journal of Advanced Manufacturing Technology 2012 67:1, 67(1), 811–21, 2012. https://doi.org/10.1007/S00170-012-4525-1

[21] N. Panwar and A. Chauhan, Development of aluminum composites using Red mud as reinforcement- A review, in: 2014 Recent Advances in Engineering and Computational Sciences (RAECS), IEEE, 2014, pp. 1–4

[22] J.A.K. Gladston, N.M. Sheriff, I. Dinaharan, and J.D. Raja Selvam, Production and characterization of rich husk ash particulate reinforced AA6061 aluminum alloy composites by compocasting. Transactions of Nonferrous Metals Society of China (English Edition), 25(3), 683–91, 2015. https://doi.org/10.1016/S1003-6326(15)63653-6

[23] B.P. Kumar and A.K. Bırru, Microstructure and mechanical properties of aluminium metal matrix composites with addition of bamboo leaf ash by stir casting method. Transactions of Nonferrous Metals Society of China (English Edition), 27(12), 2555–72, 2017. https://doi.org/10.1016/S1003-6326(17)60284-X

[24] K.S.S. Raja, V.K.B. Raja, K.R. Vignesh, and S.N.R. Rao, Effect of Steel Slag on the Impact Strength of Aluminium Metal Matrix Composite. Applied Mechanics and Materials, 766–767, 240–5, 2015. https://doi.org/10.4028/www.scientific.net/AMM.766-767.240

[25] K.S. Sridhar Raja, V.K. Bupesh Raja, and M. Gupta, Using Anthropogenic Waste (Steel Slag) To Enhance Mechanical and Wear Properties of A Commercial Aluminium Alloy A356. Arch. Metall. Mater, 64(1), 279–84, 2019. https://doi.org/10.24425/amm.2019.126249

[26] R.N. Prabu, Taguchi Method Analysis of Machining Properties of Al- Slag / Flyash Hybrid Composite. Turkish Journal of Computer and Mathematics Education, 11(03), 1596–603, 2020

[27] I.N. Murthy, N.A. Babu, and J.B. Rao, Comparative Studies on Microstructure and Mechanical Properties of Granulated Blast Furnace Slag and Fly Ash Reinforced AA 2024 Composites. Journal of Minerals and Materials Characterization and Engineering, 02(04), 319–33, 2014. https://doi.org/10.4236/jmmce.2014.24037

[28] K.S.S. Kumar, K.V. Rao, K. Anjaneyulu, and C. Ramakrıshna, Study On Material Properties of Aluminum With Silicon Carbide And Blast Furnace Slag. Anveshana's International Journal of Research in Engineering and Applied Sciences, 3(2), 207–13, 2018

[29] G. Siva Karuna, S.V.G. Swamy, and G.S. Naidu, Effect of Blast Furnace Slag and Red Mud Reinforcements on the Mechanical Properties of AA2024 Hybrid Composites. Advanced Materials Research, 1148, 29–36, 2018. https://doi.org/10.4028/www.scientific.net/amr.1148.29

[30] N. Ashrafi, A.H. Mohamed Ariff, D. Jung, M. Sarraf, J. Foroughi, S. Sulaiman, and T.S. Hong, Magnetic, Electrical, and Physical Properties Evolution in Fe3O4 Nanofiller Reinforced Aluminium Matrix Composite Produced by Powder Metallurgy Method. Materials, 15(12), 4153, 2022. https://doi.org/10.3390/ma15124153

[31] L.-M.-P. Ferreira, E. Bayraktar, I. Miskioglu, and M.-H. Robert, New magnetic aluminum matrix composites (Al-Zn-Si) reinforced with nano magnetic Fe 3 O 4 for aeronautical applications. Advances in Materials and Processing Technologies, 4(3), 358–69, 2018. https://doi.org/10.1080/2374068X.2018.1432940

[32] S. a, R. Subramanya, and Y. Basavaraj, Tensile hardness and wear properties of iron oxide (Fe3O4) reinforced aluminium 7075 metal matrix composites. Advances in Materials and Processing Technologies, 00(00), 1–15, 2022. https://doi.org/10.1080/2374068X.2022.2079227

[33] L.-M.-P. Ferreira, E. Bayraktar, M.-H. Robert, and I. Miskioglu, Optimization of Magnetic and Electrical Properties of New Aluminium Matrix Composite Reinforced with Magnetic Nano Iron Oxide (Fe3O4), in: C. Ralph, M. Silberstein, P. R. Thakre, R. Singh (Eds.), Conference Proceedings of the Society for

Experimental Mechanics Series, Vol. 7, Springer International Publishing, Cham, 2016, pp. 11–8

[34] L.-M.-P. Ferreira, E. Bayraktar, and M.-H. Robert, Magnetic and electrical properties of aluminium matrix composite reinforced with magnetic nano iron oxide (Fe 3 O 4). Advances in Materials and Processing Technologies, 2(1), 165–73, 2016. https://doi.org/10.1080/2374068X.2016.1164529

[35] E. Bayraktar and D. Katundi, Development of a new aluminium matrix composite reinforced with iron oxide (Fe 3 O 4). Journal of Achievements in Materials and Manufacturing Engineering, 38(1), 7–14, 2010

[36] E. Bayraktar, F. Ayari, M.J. Tan, A. Tosun-Bayraktar, and D. Katundi, Manufacturing of Aluminum Matrix Composites Reinforced with Iron Oxide (Fe3O4) Nanoparticles: Microstructural and Mechanical Properties. Metallurgical and Materials Transactions B, 45(2), 352–62, 2014. https://doi.org/10.1007/s11663-013-9970-1

[37] E. Mahmoud and M. Tash, Characterization of Aluminum-Based-Surface Matrix Composites with Iron and Iron Oxide Fabricated by Friction Stir Processing. Materials, 9(7), 505, 2016. https://doi.org/10.3390/ma9070505

[38] E. Bayraktar, F. Ayari, M. Jen Tan, A. Tosun-bayraktar, and D. Katundi, Manufacturing of Aluminum Matrix Composites Reinforced with Iron Oxide (Fe 3 O 4) Nanoparticles: Microstructural and Mechanical Properties. n.d. https://doi.org/10.1007/s11663-013-9970-1

[39] M.C. Şenel and M. Gürbüz, Partikül Boyutunun ve B4C Katkı Oranının Al-B4C Kompozitlerin Mekanik ve Mikroyapı Özellikleri Üzerine Olan Etkisi. Düzce Üniversitesi Bilim ve Teknoloji Dergisi, 8, 1864–76, 2020. https://doi.org/10.29130/dubited.683876

[40] M. Toozandehjani, K.A. Matori, F. Ostovan, K.R. Jamaludin, A. Amrin, and E. Shafiei, The Effect of the Addition of CNTs on the Microstructure, Densification and Mechanical Behavior in Al-CNT-Al2O3 Hybrid Nanocomposites. JOM, 72(6), 2283–94, 2020. https://doi.org/10.1007/s11837-020-04132-5

[41] G. Tosun and M. Kurt, The porosity, microstructure, and hardness of Al-Mg composites reinforced with micro particle SiC/Al2O3 produced using powder metallurgy. Composites Part B: Engineering, 174, 106965,2019.https://doi.org/10.1016/j.compositesb.2019.106965

[42] E. Özer, M. Ayvaz, M. Übeyli, and İ. Sarpkaya, Properties of Aluminum Nano Composites Bearing Alumina Particles and Multiwall Carbon Nanotubes Manufactured by Mechanical Alloying and Microwave Sintering. Metals and Materials International, 1–18, 2022. https://doi.org/10.1007/s12540-022-01238-0

[43] M. Toozandehjanı, F. Ostovan, K.R. Jamaludın, A. Amrın, K.A. Matorı, and E. Shafıeı, Process−microstructure−properties relationship in Al−CNTs−Al2O3 nanocomposites manufactured by hybrid powder metallurgy and microwave sintering process. Transactions of Nonferrous Metals Society of China, 30(9), 2339–54, 2020. https://doi.org/10.1016/S1003-6326(20)65383-3

[44] H. Kwon, M. Estili, K. Takagi, T. Miyazaki, and A. Kawasaki, Combination of hot extrusion and spark plasma sintering for producing carbon nanotube reinforced aluminum matrix composites. Carbon, 47(3), 570–7, 2009. https://doi.org/10.1016/j.carbon.2008.10.041

[45] E. Tekoğlu, D. Ağaoğulları, Y. Yürektürk, B. Bulut, and M. Lütfi Öveçoğlu, Characterization of LaB6 particulate-reinforced eutectic Al-12.6 wt% Si composites fabricated via mechanical alloying and spark plasma sintering. Powder Technology, 340, 473–83, 2018. https://doi.org/10.1016/j.powtec.2018.09.055

[46] U. Çavdar, Energy Consumption Analysis of Sintering Temperature Optimization of Pure Aluminum Powder Metal Compacts Sintered by Using The UHFIS. Uluslararası Muhendislik Arastirma ve Gelistirme Dergisi, (December 2018), 174–85, 2017. https://doi.org/10.29137/umagd.348072

[47] V. Chak, H. Chattopadhyay, and T.L. Dora, A review on fabrication methods, reinforcements and mechanical properties of aluminum matrix composites. Journal of Manufacturing Processes, 56(May 2019), 1059–74, 2020. https://doi.org/10.1016/j.jmapro.2020.05.042

[48] R.M. German, P. Suri, and S.J. Park, Review: liquid phase sintering. Journal of Materials Science, 44(1), 1–39, 2009. https://doi.org/10.1007/s10853-008-3008-0

[49] C. Borgohain, K. Acharyya, S. Sarma, K.K. Senapati, K.C. Sarma, and P. Phukan, A new aluminum-based metal matrix composite reinforced with cobalt ferrite magnetic nanoparticle. Journal of Materials Science, 48(1), 162–71, 2013. https://doi.org/10.1007/s10853-012-6724-4

[50] A. Maleki, A.R. Taherizadeh, H.K. Issa, B. Niroumand, A.R. Allafchian, and A. Ghaei, Development of a new magnetic aluminum matrix nanocomposite. Ceramics International, 44(13), 15079–85, 2018. https://doi.org/10.1016/j.ceramint.2018.05.141

[51] R. Calin, M. Pul, and Z.O. Pehlivanli, The effect of reinforcement volume ratio on porosity and thermal conductivity in Al-Mgo composites. Materials Research, 15(6), 1057–63, 2012. https://doi.org/10.1590/S1516-14392012005000131

[52] M. Cabeza, I. Feijoo, P. Merino, G. Pena, M.C. Pérez, S. Cruz, and P. Rey, Effect of high energy ball milling on the morphology, microstructure and properties of nano-sized TiC particle-reinforced 6005A aluminium alloy matrix composite. Powder Technology, 321, 31–43, 2017.https://doi.org/10.1016/j.powtec.2017.07.089

[53] S. Aktaş and E. Anıl Diler, Effect of ZrO2 Nanoparticles and Mechanical Milling on Microstructure and Mechanical Properties of Al–ZrO2 Nanocomposites. Journal of Engineering Materials and Technology, 143(4), 2021. https://doi.org/10.1115/1.4050726

[54] C.F. Deng, D.Z. Wang, X.X. Zhang, and A.B. Li, Processing and properties of carbon nanotubes

reinforced aluminum composites. Materials Science and Engineering: A, 444(1–2), 138–45, 2007. https://doi.org/10.1016/j.msea.2006.08.057

[55] J.B. Fogagnolo, E.M. Ruiz-Navas, M.H. Robert, and J.M. Torralba, The effects of mechanical alloying on the compressibility of aluminium matrix composite powder. Materials Science and Engineering: A, 355(1–2), 50–5, 2003. https://doi.org/10.1016/S0921-5093(03)00057-1

[56] K. Ozturk, R. Gecu, and A. Karaaslan, Microstructure, wear and corrosion characteristics of multiple-reinforced (SiC–B4C–Al2O3) Al matrix composites produced by liquid metal infiltration. Ceramics International, 47(13), 18274–85, 2021. https://doi.org/10.1016/j.ceramint.2021.03.147

[57] J. Li, Y. Lu, H. Zhang, and L. Xin, Effect of grain size and hardness on fretting wear behavior of Inconel 600 alloys. Tribology International, 81, 215–22, 2015. https://doi.org/10.1016/j.triboint.2014.08.005

[58] A. Mazahery and M.O. Shabani, Microstructural and abrasive wear properties of SiC reinforced aluminum-based composite produced by compocasting. Transactions of Nonferrous Metals Society of China, 23(7), 1905–14, 2013. https://doi.org/10.1016/S1003-6326(13)62676-X.